

Research Article

Mutual Coupling Reduction Using a Protruded Ground Branch Structure in a Compact UWB Owl-Shaped MIMO Antenna

A. Mchbal , N. Amar Touhami, H. Elftouh, and A. Dkiouak

Physics Department, Information Systems and Telecommunications Laboratory, Faculty of Sciences, Abdelmalek Essaadi University, Tetouan, Morocco

Correspondence should be addressed to A. Mchbal; aicha.mchbal8@gmail.com

Received 21 March 2018; Revised 16 June 2018; Accepted 12 July 2018; Published 4 September 2018

Academic Editor: Jaume Anguera

Copyright © 2018 A. Mchbal et al. This is an open access article distributed under the Creative Commons Attribution License, which permits unrestricted use, distribution, and reproduction in any medium, provided the original work is properly cited.

A compact ultra-wideband (UWB) multiple input-multiple output (MIMO) antenna with high isolation is designed for UWB applications. The proposed MIMO antenna consists of two identical monopole antenna elements. To enhance the impedance matching, three slots are formed on the ground plane. The arc structure as well as the semicircle with an open-end slot is employed on the radiating elements the fact which helps to extend the impedance bandwidth of the monopole antenna from 3.1 up to 10.6 GHz, which corresponds to the UWB band. A ground branch decoupling structure is introduced between the two elements to reduce the mutual coupling. Simulation and measurement results show a bandwidth range from 3.1 to 11.12 GHz with $|S_{11-}| < -15$ dB, $|S_{21-}| < -20$ dB, and $ECC < 0.002$.

1. Introduction

UWB technology has been developed rapidly since FCC assigned a range of 3.1–10.6 GHz for UWB applications in 2002 [1]. The UWB communication system is well known for its fundamental advantages, which are low power and high data interference immunity [2]. However, one significant issue with this system is multipath fading, which is considered to be a prominent factor that affects the communication reliability of multisignals as well as the efficiency of an UWB system [3, 4]. Thus, to overcome this problem, MIMO has been introduced as an efficient technique to improve the UWB system performance.

MIMO technology has caught our attention as it significantly increased channel capacity without any additional power or bandwidth [5, 6]; however, we have found the mutual coupling between the UWB antenna elements which are very large to get installed on a confined space with the multiple antenna elements. It means that, if the MIMO antenna elements were placed very close to each other, there would be a strong correlation between their signals and the utility of MIMO would be reduced, so the mutual coupling is inversely proportional to the separation between the

antenna elements. Thus, it is a challenge to design an UWB MIMO antenna with extremely compact structures and that have a low mutual coupling [7, 8]. We can say that the most critical point that must be considered while designing a MIMO antenna is to attain a low mutual coupling amid adjacent radiating elements because the MIMO antenna system performance can be strongly affected by the mutual coupling between the MIMO antenna elements, which considerably alter impedance matching, radiation efficiency, and channel capacity [9].

Based on the previous reasons, it is necessary to design UWB MIMO antennas with high isolation between their elements. Therefore, various techniques have been applied for the improvement of isolation amid closely spaced antennas, and several approaches have also been used to diminish the mutual coupling between the antenna elements. They include electromagnetic band gap (EBG) structures, defected ground structures (DGS), orthogonal polarization, placing metal strips between elements, metasurfaces, and neutralization line technique [10–14].

In [11], a high isolation MIMO antenna was designed for UWB applications and was exposed; between two of its elements, a comb-line structure was inserted in order to

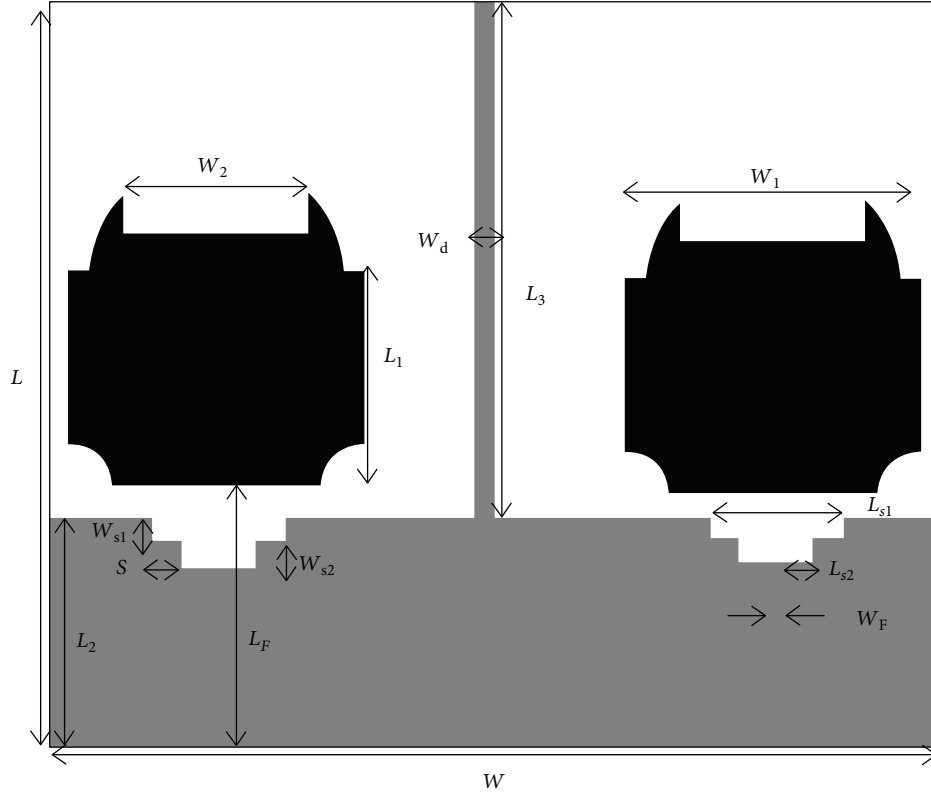


FIGURE 1: Structure of the proposed antenna.

achieve high isolation. In [15], an UWB MIMO antenna was proposed with two rejected bands to avoid the interference between UWB applications and narrow band “ones.” In [16], MIMO antenna elements were placed vertically to minimize mutual coupling, and four notched bands were achieved by inserting symmetrical L-shaped slots and C-shaped stubs in each element. In [17], two MIMO configurations were discussed. In the first one, the antenna elements were placed side by side with a separated ground plane. In the second configuration, the antenna elements were orthogonally placed and had a separated ground plane as well.

The UWB MIMO antenna in [18] could achieve a mutual coupling larger than 20 dB in the entire operating band by etching a T-shaped slot as well as a narrow slot on the ground plane. In [12], a miniaturized MIMO antenna has been proposed for industrial applications, which had a novel decoupling stub structure etched in the ground plane to improve isolation between the antenna elements over the complete frequency band.

In [19], the developed MIMO antenna consists of a pair of rectangular patch elements, with staircase truncations at the patch-feed interconnection. DGS techniques as well as arc-shaped and split ring slots were used to obtain two band notches. In [13], two circular disc monopole antenna elements were designed for the proposed UWB-MIMO antenna. The mutual coupling between the two elements has been enhanced by using an inverted Y-shaped stub on the ground plane, which helps to miniaturize the antenna.

TABLE 1: Dimensions of the proposed antenna in (mm).

L	L_1	L_2	L_3	L_F	L_{s1}	L_{s2}	W	W_1	W_2
31	8.3	8	18	9	4	1	26	11	6
W_d	W_F	W_{s1}	W_{s2}	S	S_1	R	R_1	T	H
1	1	0.8	1	0.5	1	2.5	4.6	0.035	0.8

In this paper, an UWB antenna with high isolation characteristics is presented. The MIMO antenna uses two monopole antenna elements with a compact size of $8.3 \times 11 \text{ mm}^2$ in each. An arc structure as well as an open-end slot is formed in the radiating elements in order to cover a wide bandwidth for UWB applications.

A ground branch decoupling structure was used to minimize the coupling between the radiating elements. A bandwidth of 3.1–11.12 GHz is covered, and high isolation, of more than -19 dB on the entire band, is achieved.

2. Proposed Antenna Design

The antenna is mounted on a $26 \times 31 \times 0.8 \text{ mm}^3$ FR-4 substrate with a dielectric constant $\epsilon_r = 4.3$ and a loss tangent of 0.0027. Figure 1 exhibits the geometry of the UWB MIMO antenna.

There are two similar owl-shaped radiating elements with a size of (W_1, L_1) in the system. A partial ground plane (L_2, W) is used with three slots with dimensions $(W_{s1}, L_{s1}, L_{s2}, W_{s2})$ to improve impedance matching. An arc structure

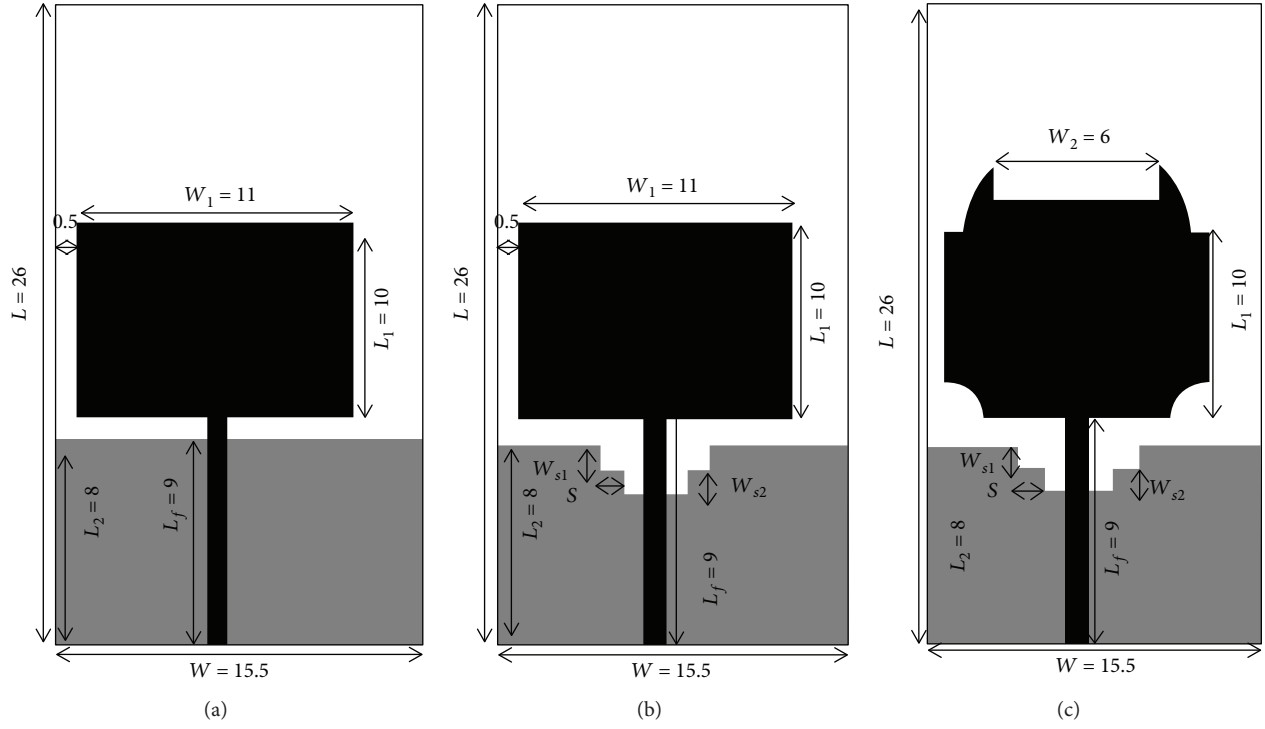


FIGURE 2: (a) Configuration of antenna 1. (b) Configuration of antenna 2. (c) Configuration of antenna 3.

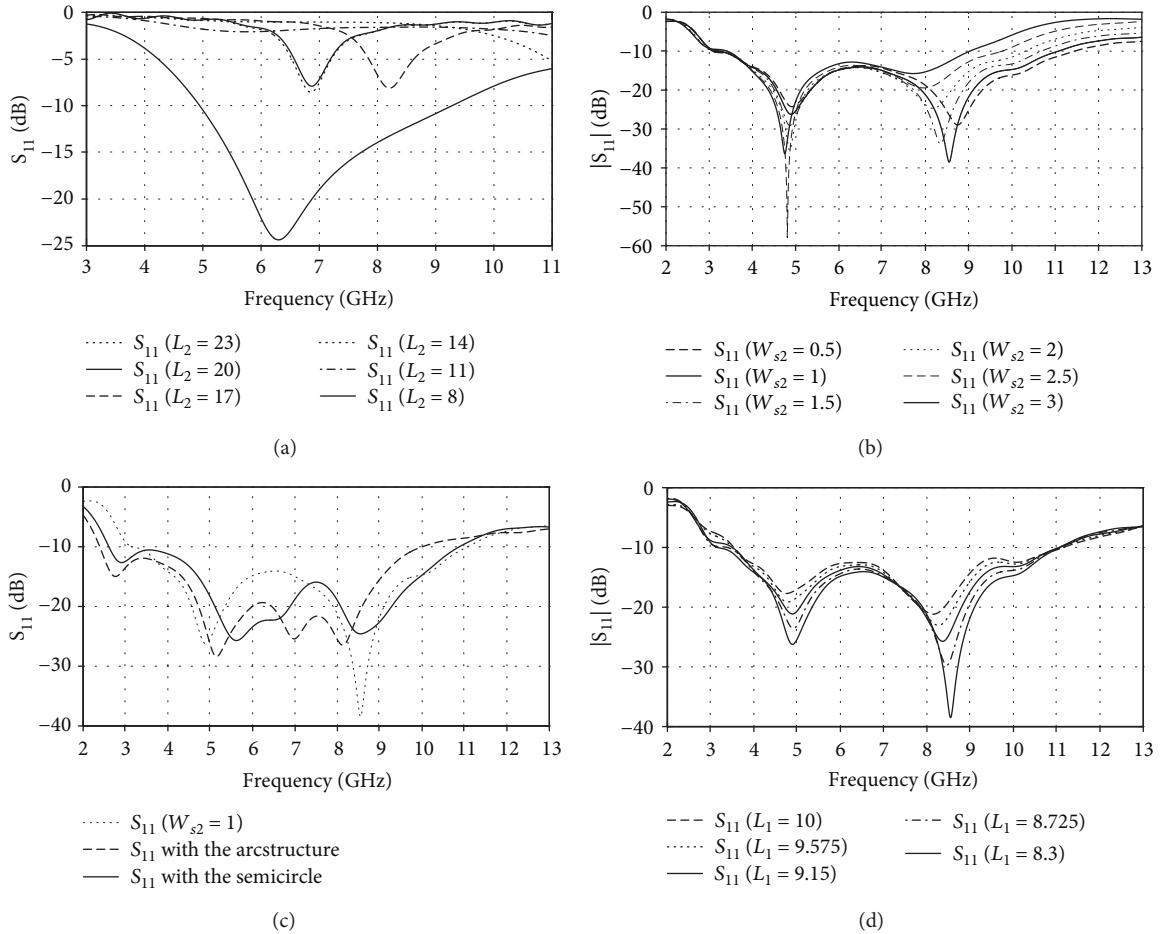
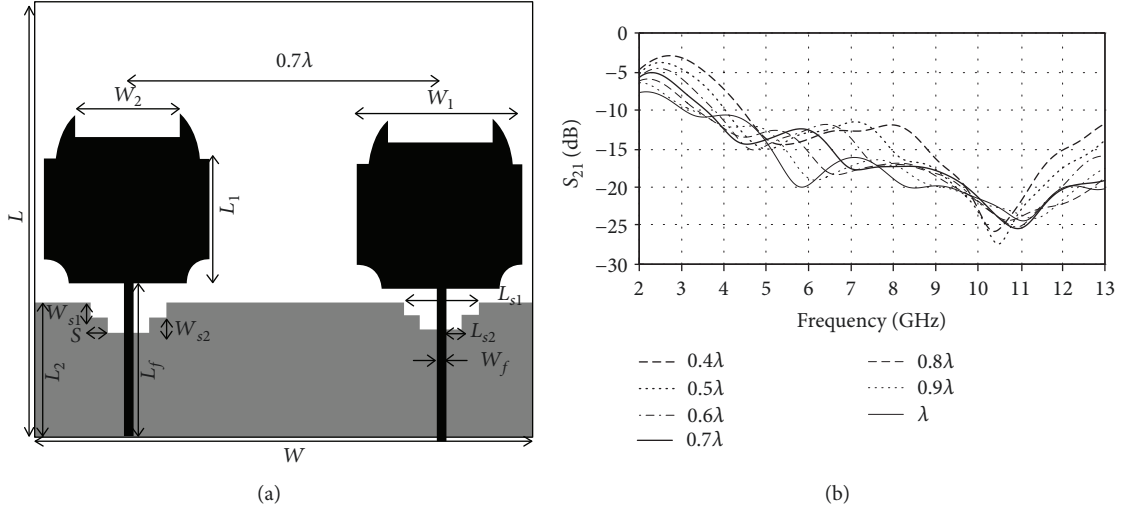
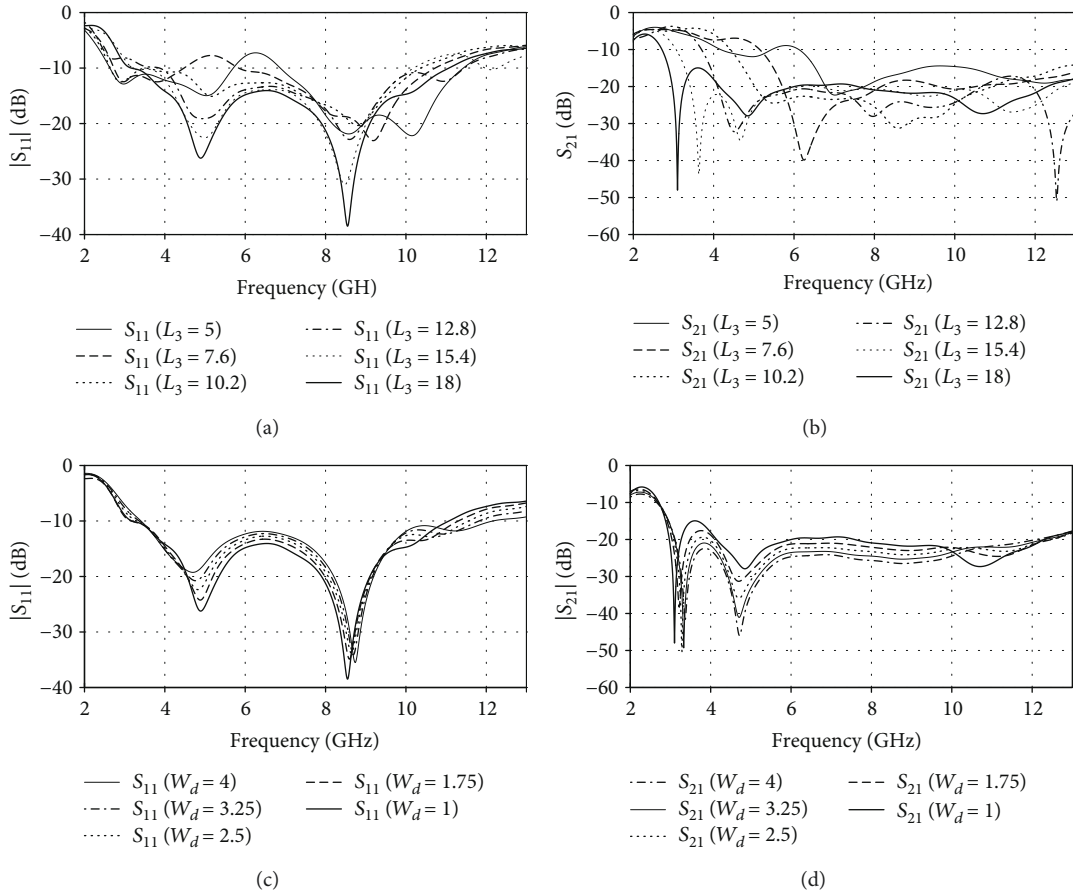


FIGURE 3: (a) $|S_{11}|$ of antenna 1. (b) $|S_{11}|$ of antenna 2. (c) $|S_{11}|$ of antenna 3. (d) $|S_{11}|$ with varying L_2 .

FIGURE 4: (a) MIMO antenna I. (b) S_{21} with varying D .FIGURE 5: (a, b) $|S_{11}|$ and $|S_{21}|$ of MIMO antenna with decoupling structure with varying L_3 . (c, d) $|S_{11}|$ and $|S_{21}|$ of MIMO antenna with decoupling structure with varying W_d .

(R) is formed on the two corners of radiating elements in order to shift the frequency to a lower one.

Finally, a semicircle (R_1) with an open-ended slot (R_2) is applied on the two elements to cover the entire UWB frequency band. The radiating elements are fed by a microstrip line with dimensions (W_F , L_F).

The final step on the design of our antenna was to apply a decoupling structure with dimensions (W_d , L_3) in the ground plane in order to reduce the mutual coupling between the elements. Computer Simulation Technology (CST) Microwave Studio Software is used to simulate the proposed antenna.

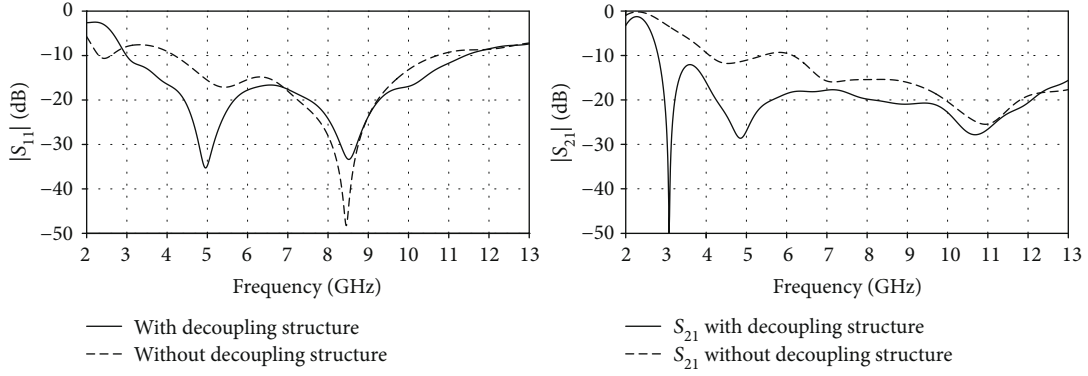


FIGURE 6: Simulated S-parameters.

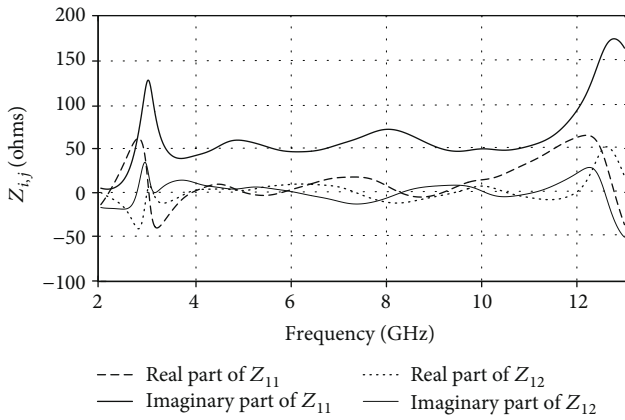


FIGURE 7: Simulated input impedance of the proposed MIMO antenna.

After performing several simulations using CST MWS, the optimized parameters of the proposed UWB antenna are listed in Table 1.

3. Discussion of Design Process

The described MIMO antenna in Figure 1 is constructed by joining two UWB monopole antenna elements. This design has been chosen because of its attractive characteristics, which are simple structure, omnidirectional radiation pattern, low profile, and wide bandwidth. The frequency corresponding to the resonance of a rectangular planar monopole antenna can be approximately calculated by [20]

$$F_{r1} = \frac{144}{L_2 + L_1 + g + (w/2\pi\sqrt{1 + \epsilon_r}) + (w/2\pi\sqrt{1 + \epsilon_r})} \text{ GHz.} \quad (1)$$

where L_2 and L_1 denote the length of the ground plane and the monopole antenna, respectively, and g is the gap between them. According to Formula (1), the calculated F_{r1} is 6.8 GHz, which corresponds to the center frequency of an UWB band. The dimensions of the initial monopole antenna structure have been chosen to obtain a resonant frequency of 6.8 GHz which represents the center frequency of an UWB since our purpose is to design a MIMO antenna for UWB applications. Figure 2 shows the single

element of our proposed MIMO antenna. The simulated $|S_{11}|$ is less than -10 dB across the whole band which is due to the compact size of the antenna elements and the ground plane. Therefore, in order to shift the resonant frequency to get it lower and improve the impedance matching, a modification is applied on the ground plane by changing its length L_2 . The obtained results in $|S_{11}|$ implies that the partial ground plane has a significant effect on the input impedance matching, as shown in Figure 3(a), which represents the $|S_{11}|$ with varying the length of the ground plane.

On the other hand, by placing the two antenna elements close to each other, the bandwidth still cannot cover the entire UWB, so to shift the resonant frequency of the low band to a lower one, three small rectangular slots are cut on the ground plane, as well as by changing W_{s2} from 3 to 1 mm, the lower frequency is shifted from more than 4 GHz to about 3 GHz as shown in Figure 3(b).

Moreover, by forming an arc structure on the two corners of the two antenna elements as well as by applying a semicircle with an open-end slot on them, a good impedance matching is obtained across the whole UWB frequency band as it is shown in Figure 3(c).

Finally, by decreasing the value of the length of the radiating elements (L_1) from 10 to 8.3 mm, a bandwidth of 3.1–11.12 is covered.

4. Isolation Improvement

The described MIMO antenna in Figure 4(a) is constructed by joining two UWB monopole antenna elements, which are placed side by side, a distance D from each other, with a common ground plane. Since the ground plane is very compact, the surface current and the near-field radiation cause strong mutual coupling between the UWB antennas, which leads to a signal interference that limits the MIMO system efficiency.

In order to improve isolation, several simulations and parametric studies were performed to obtain the optimum distance between the antenna elements. Figure 4(b) illustrates a parametric study of S_{21} as a function of λ .

Results show that with $D = 0.7\lambda$, the antenna elements achieve better isolation. As shown above, isolation can be

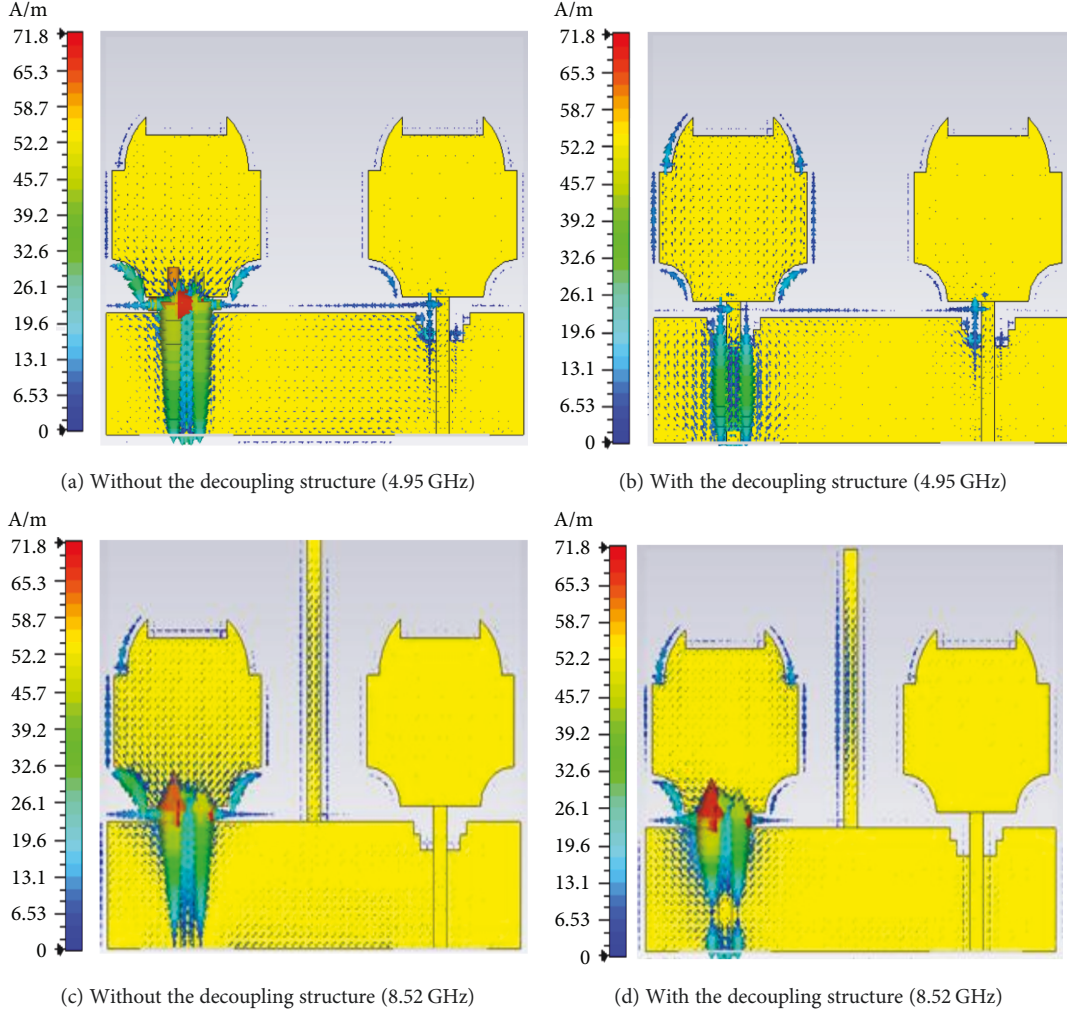


FIGURE 8: Current distribution of the proposed antenna.

easily improved by increasing the distance between the antenna elements, but the compact size of the wireless devices limits this approach.

Therefore, a good challenge has appeared, meaning, in order to enhance isolation or to reduce the mutual coupling by using some other technique. Among these techniques, we can find the implementation of a decoupling structure between the antenna elements.

Figure 1 depicts our proposed antenna with a decoupling structure that is well known in the literature by a protruded ground branch.

As shown in Figures 5(a) and 5(b), as L_3 increases and W_d decreases, the isolation is improved significantly while a good impedance matching is maintained across the UWB frequency band. Figure 5 represents the S -parameters of the proposed MIMO antenna with a variation in the length (L_3) and the width (W_d) of the decoupling structure.

The main objective of introducing the stub on the ground plane of the antenna is to enhance the isolation between the ports of the constituent radiating elements; therefore, its significance can be evaluated by observing

the S -parameters of the proposed UWB MIMO antenna, comparing them with those that are without a stub.

Figure 6 shows the simulated S -parameters of the developed UWB MIMO antenna with and without the decoupling structure.

The final step when the final antenna is designed with the optimized dimensions is to simulate the input impedance of our proposed antenna, in order to check the adaptation. Figure 7 illustrates the Z -parameters of our proposed antenna. So, as we can see in Figure 7, the adaptation is attained over the whole UWB band.

To further understand the effects of the decoupling structure on the mutual coupling between the antenna elements, Figure 8 shows the current distribution of our proposed antenna with and without using the decoupling structure which is obtained by exciting port 1.

The current is mainly concentrated on the feed line of the excited element, while a significant amount of current is flowing through the decoupling structure between the two elements of our proposed antenna which nullifies radiation. So the coupling between the antennas is minimized.

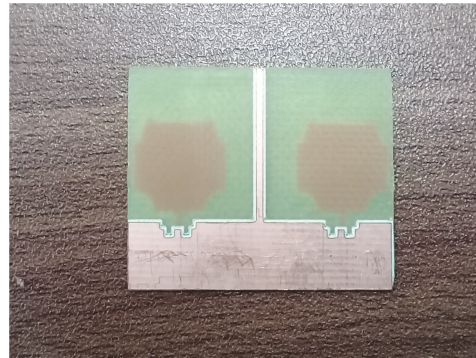
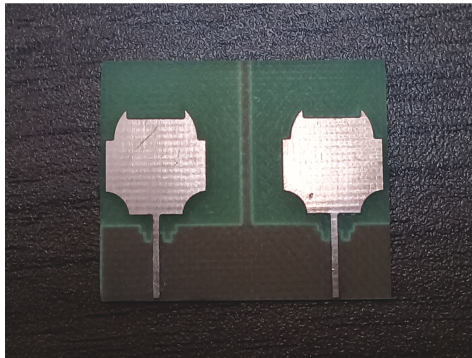
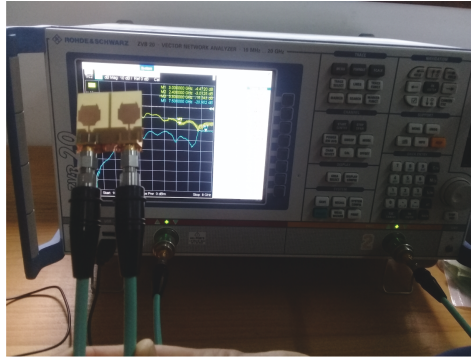


FIGURE 9: Photographs of the fabricated antenna.

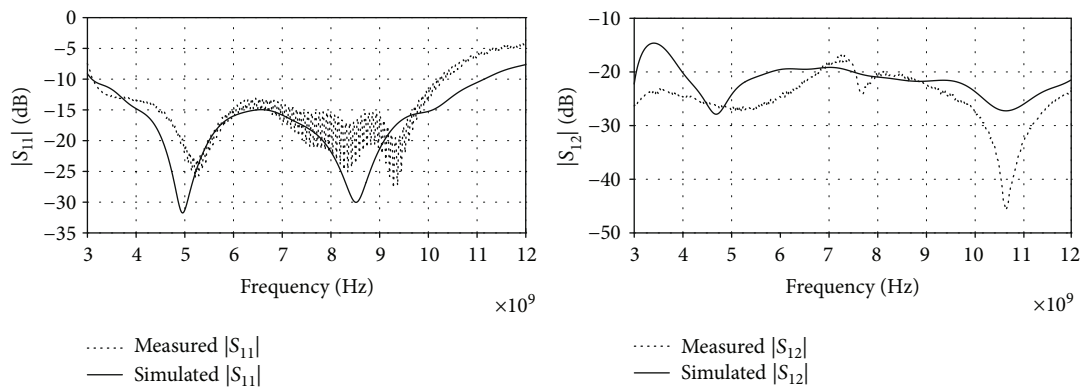


FIGURE 10: The measured and simulated S-parameters of the proposed antenna.

5. Results and Discussions

The Rohde and Schwarz ZVB 20 vector network analyzer is used to measure the proposed antenna S-parameters by connecting port 1 and port 2 with two SMA female connectors. The photographs of the fabricated UWB MIMO antenna are shown in Figure 9.

The results indicate that our antenna is giving a good impedance bandwidth with both measured and simulated S-parameters; $S_{11} < -15$ dB from 3.1–11.12 GHz and S_{12} are less than -20 dB throughout the ultra-wideband. Figure 10 illustrates the simulated and measured S-parameters.

5.1. Radiation Patterns. It is clear that the xz -plane corresponds to the H -plane and the yz -plane corresponds to the E -plane. The radiation patterns are obtained by using an

active element pattern. It means the radiation patterns of a single element, when the other one is presented but is not excited. It is also known as an embedded element pattern. The simulated and measured E -plane and H -plane radiation patterns of the proposed antenna are illustrated in Figure 11.

As we can see, as the frequency increases, the radiation pattern gets distorted. Note that the radiation patterns in the H -plane as well as in the E -plane are omnidirectional to receive the signals from all directions.

The difference between the simulated and the measured radiation patterns of the H -plane occurs because the measurement is not carried out in an anechoic chamber.

5.2. Envelope Correlation Coefficient. The envelope correlation coefficient presents an important factor for the comparison of MIMO capabilities of coupled antennas.

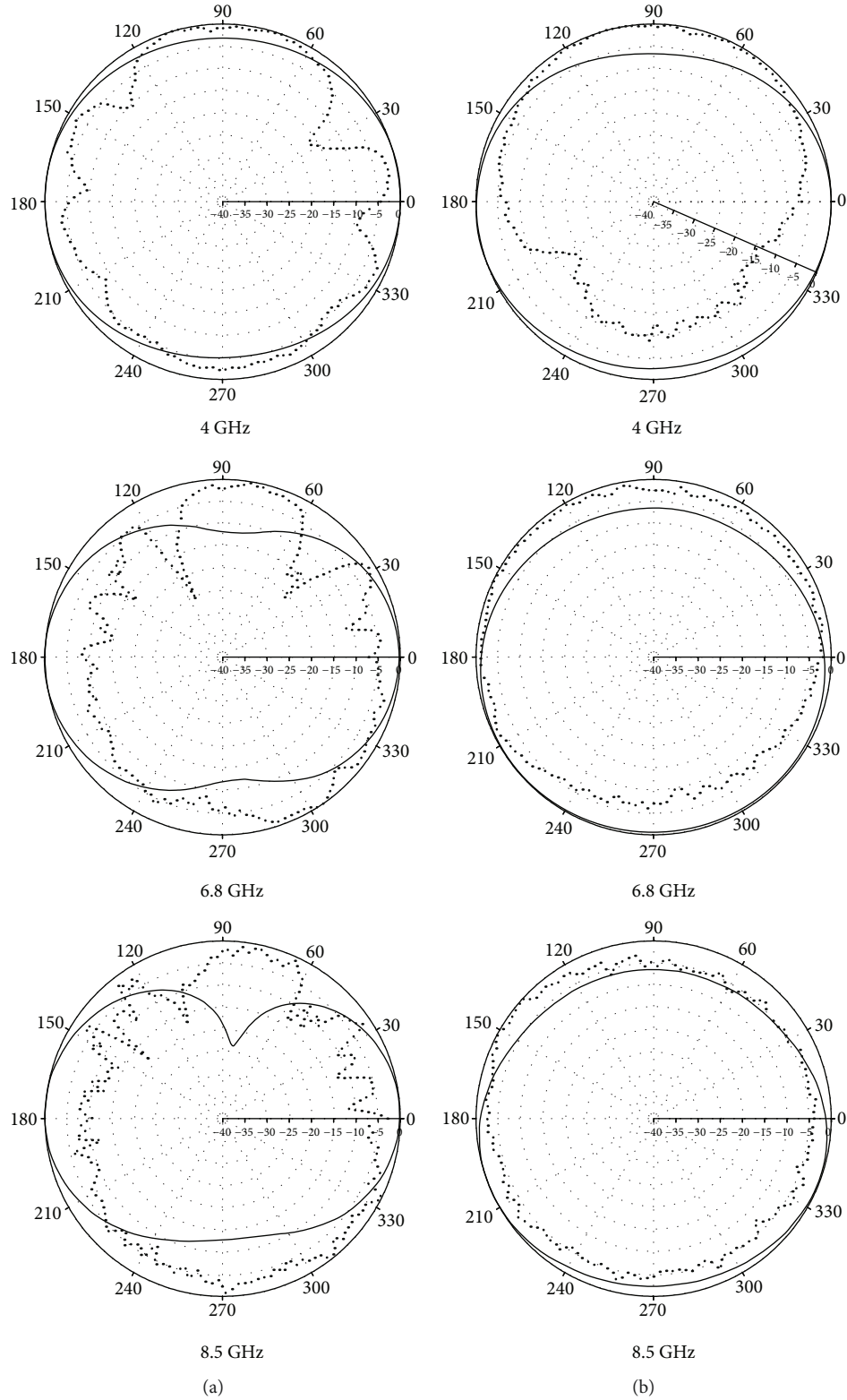


FIGURE 11: The measured and simulated radiation patterns of the proposed MIMO antenna. (a) H -plane. (b) E -plane.

In general, there are three methods to calculate the envelope correlation coefficient. The first one consists of using far-field pattern data, which is considered to be a method that consumes much time because of its computational complexity.

The second method is based on Clarke's formula, while the third one employs the scattering parameter formulation which can reduce the calculation complexity using the other methods. The last method can easily be generalized to the envelope correlation of a system with N -antenna [21].

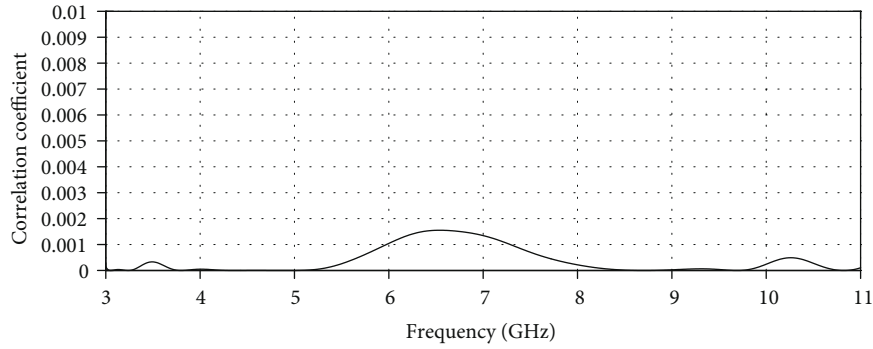


FIGURE 12: Simulated envelope correlation coefficient.

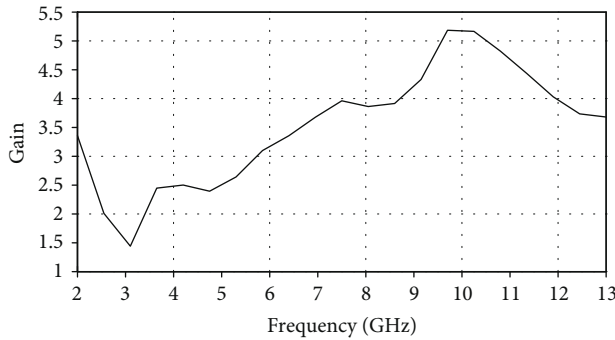


FIGURE 13: Simulated gain.

So in order to have a better evaluation of MIMO diversity characteristic, an easy formula to compute ECC is provided:

$$ECC = \frac{|S_{11}^* S_{12}^* + S_{21}^* S_{22}^*|^2}{(1 - |S_{11}|^2 - |S_{21}|^2)(1 - |S_{22}|^2 - |S_{21}|^2)}. \quad (2)$$

Based on the measured S-parameters, using Formula (2), and comparing it with the simulated one depicted in Figure 12, we obtained a result that showed that the ECC is less than 0.002 from 3.1–11.2 GHz which demonstrates the diversity good performance.

As it is shown in Figure 13, the value of the simulated gain of the proposed MIMO antenna has ranged from 2.5 to 5.54 over the UWB frequency band.

6. Conclusion

A novel compact owl-shaped UWB MIMO antenna is presented in this paper. Three slots were etched on the ground plane to improve impedance matching of the radiating elements to better than -15 dB. An arc structure as well as an open-end slot were applied on the radiating elements in order to cover the whole UWB band. A protruded ground branch was introduced in between the antenna elements to decrease the mutual coupling; a high isolation of less than -20 dB across the whole band was achieved.

Good radiation performances were also obtained. An envelope correlation coefficient of less than 0.002 was achieved, and a good gain value which is restricted to an average between 2.5 and 5.54 dB was obtained.

These results prove that the proposed owl-shaped MIMO antenna is very adequate for UWB applications.

Data Availability

The data used to support the findings of this study are included in the article.

Conflicts of Interest

The authors declare that there is no conflict of interests regarding the publication of this paper.

Acknowledgments

This research was partially supported by the National School of Applied Sciences, under Sciences and Advanced Technologies Laboratory, Abdelmalek Essaadi University, Tetouan, Morocco, supervised by Professor Alia Zekriti.

References

- [1] S. Saxena, B. K. Kanaujia, S. Dwari, S. Kumar, and R. Tiwari, "A compact dual-polarized MIMO antenna with distinct diversity performance for UWB applications," *IEEE Antennas and Wireless Propagation Letters*, vol. 16, pp. 3096–3099, 2017.
- [2] D. Yadav and V. Tiwari, "UWB Antenna Designing: Challenges and Solutions," *International Journal of Computing, Communication and Instrumentation Engineering*, vol. 1, no. 1, 2014.
- [3] J.-F. Li, Q.-X. Chu, Z.-H. Li, and X.-X. Xia, "Compact dual band-notched UWB MIMO antenna with high isolation," *IEEE Transactions on Antennas and Propagation*, vol. 61, no. 9, pp. 4759–4766, 2013.
- [4] D.-G. Kang, J. Tak, and J. Choi, "MIMO antenna with high isolation for WBAN applications," *International Journal of Antennas and Propagation*, vol. 2015, Article ID 370763, 7 pages, 2015.
- [5] S. Soltani and R. D. Murch, "A compact planar printed MIMO antenna design," *IEEE Transactions on Antennas and Propagation*, vol. 63, no. 3, pp. 1140–1149, 2015.
- [6] L. Yang, T. Li, and S. Yan, "Highly compact MIMO antenna system for LTE/ISM applications," *International Journal of Antennas and Propagation*, vol. 2015, Article ID 714817, 10 pages, 2015.

- [7] S. Shoaib, I. Shoaib, N. Shoaib, X. Chen, and C. G. Parini, "MIMO antennas for mobile handsets," *IEEE Antennas and Wireless Propagation Letters*, vol. 14, pp. 799–802, 2015.
- [8] Z. Yang, H. Yang, and H. Cui, "A compact MIMO antenna with inverted C-shaped ground branches for mobile terminals," *International Journal of Antennas and Propagation*, vol. 2016, Article ID 3080563, 6 pages, 2016.
- [9] Q. Zeng, Y. Yao, S. Liu, J. Yu, P. Xie, and X. Chen, "Tetraband small-size printed strip MIMO antenna for mobile handset application," *International Journal of Antennas and Propagation*, vol. 2012, Article ID 320582, 8 pages, 2012.
- [10] G.-S. Lin, C.-H. Sung, J.-L. Chen, L.-S. Chen, and M.-P. Hwang, "Isolation improvement in UWB MIMO antenna system using carbon black film," *IEEE Antennas and Wireless Propagation Letters*, vol. 16, pp. 222–225, 2017.
- [11] N. Malekpour and M. A. Honarvar, "Design of high-isolation compact MIMO antenna for UWB application," *Progress In Electromagnetics Research*, vol. 62, pp. 119–129, 2016.
- [12] M. Khan, M. Shafique, A.-D. Capobianco, E. Autizi, and I. Shoaib, "Compact UWB-MIMO antenna array with a novel decoupling structure," in *Proceedings of 2013 10th International Bhurban Conference on Applied Sciences & Technology (IBCAST)*, pp. 347–350, Islamabad, Pakistan, January 2013.
- [13] A. I. Najam, Y. Duroc, and S. Tedjini, "UWB-MIMO antenna with novel stub structure," *Progress In Electromagnetics Research C*, vol. 19, pp. 245–257, 2011.
- [14] S. Kahng, E. C. Shin, G. H. Jang, J. Anguera, J. H. Ju, and J. Choi, "A UWB antenna combined with the CRLH metamaterial UWB bandpass filter having the bandstop at the 5 GHz-band WLAN," in *2009 IEEE Antennas and Propagation Society International Symposium*, pp. 1–4, Charleston, SC, USA, June 2009.
- [15] J.-F. Li, D.-L. Wu, and Y.-J. Wu, "Dual band-notched UWB MIMO antenna with uniform rejection performance," *Progress In Electromagnetics Research*, vol. 54, pp. 103–111, 2017.
- [16] L. Wu, Y. Xia, and X. Cao, "Design of compact quad-band notched UWB-MIMO antenna," *Wireless Personal Communications*, vol. 98, no. 1, pp. 225–236, 2018.
- [17] S. A. Naser and N. I. Dib, "A compact printed UWB Pacman-shaped MIMO antenna with two frequency rejection bands," *Jordanian Journal of Computers and Information Technology*, vol. 2, no. 1, p. 1, 2016.
- [18] C. R. Jetti and V. Rao Nandanavanam, "Trident-shape strip loaded dual band-notched UWB MIMO antenna for portable device applications," *AEU - International Journal of Electronics and Communications*, vol. 83, pp. 11–21, 2018.
- [19] B. L. Prakash, B. Madhav, B. Sai Parimala, T. Sravya, and A. Tirunagari, "Dual band notch MIMO antenna with meander slot and DGS for ultra-wideband applications," *ARPJ Journal of Engineering and Applied Sciences*, vol. 12, pp. 4494–4501, 2017.
- [20] Y. Wu, K. Ding, B. Zhang, J. Li, D. Wu, and K. Wang, "Design of a compact UWB MIMO antenna without decoupling structure," *International Journal of Antennas and Propagation*, vol. 2018, Article ID 9685029, 7 pages, 2018.
- [21] Y. Dama, R. Abd-Alhameed, J. M. Noras, and N. Ali, "An exact envelope correlation formula for two-antenna systems using input scattering parameters and including power losses," *International Journal on Communications Antenna and Propagation*, vol. 2, pp. 39–44, 2012.

